International Journal of Science, Technology and Management (IJSTM) ISSN (online): 2321-774X
Volume 12, Issue 1, 2025

A Review on BLDC Motor Control and Performance Optimization for Electric Vehicle Applications

Patel Manisha Mangalbhai[1], Dr. Vineet Kumar Goel [2], Dr. Dinesh Kumar [3]

[1]Reserch Scholar, Faculty of Engineering & Technology, Bhagwan Mahavir Centre for Advance Research, BMU Campus, VIP Road, Nr. Aakash E space, Bharthana, Vesu, 395007
[2]Research Guide, Dean, Faculty of Engineering & Technology, Bhagwan Mahavir Centre for Advance Research, BMU Campus, VIP Road, Nr. Aakash E space, Bharthana, Vesu, 395007
[3]Research Coguide , Professor, JCDM College of Engineering, Sirsa, Haryana, 125055

***Abstract* - The environmental impact and fuel-related challenges associated with Internal Combustion (IC) engines have driven a global transition toward electric vehicles (EVs). As technological advancements improve the feasibility of EV adoption, Brushless DC (BLDC) motors have emerged as a preferred choice for propulsion due to their high efficiency, compactness, low maintenance, and excellent torque-speed characteristics. This paper presents a comparative overview of electric motors used in EVs, highlighting the advantages of BLDC motors over traditional DC and induction motors. It further discusses the operational principles of BLDC motors, including sensor-based and sensorless commutation techniques, and examines control strategies such as voltage variation and PWM duty cycle modulation. Particular emphasis is placed on the torque ripple issue inherent to BLDC motors and the ongoing research aimed at mitigating it to improve drive performance. The findings reinforce the suitability of BLDC motors for electric vehicle applications and emphasize the need for optimized control methods to enhance overall efficiency and dynamic response.**

Index Terms – Brushless DC (BLDC) Motor, Electric Vehicle (EV), Motor Controller Unit (MCU), Hall Sensor, PWM Control, Speed Control, Torque Ripple, Sensor-based Commutation, MATLAB Simulation and Hardware Implementation.

I. INTRODUCTION

The transportation sector has long relied on Internal Combustion (IC) engines, which, despite their widespread use and historical importance, have been significant contributors to environmental pollution due to the emission of greenhouse gases such as carbon dioxide (CO_2), carbon monoxide (CO), and other harmful byproducts. Since the early 20th century, the growing use of IC engine-powered vehicles has raised serious concerns regarding environmental sustainability and the depletion of fossil fuel resources. With increasing global population and rising living standards, the demand for energy has surged, placing further strain on fuel availability and affordability [1][2]. In response to these challenges, there has been a major shift toward alternative and sustainable transportation technologies. Electric vehicles (EVs), including Battery Electric Vehicles (BEVs) and Plug-in Hybrid Electric Vehicles (PHEVs), have gained significant momentum in recent years due to advancements in technology, improved energy efficiency, lower operational costs, and, most importantly, their environmentally friendly nature. Despite these advantages, EVs still face challenges, particularly in terms of high initial cost, primarily due to battery technologies. However, ongoing research and innovation are gradually narrowing this cost gap, making EVs increasingly viable and competitive with traditional vehicles.

A critical component of an electric vehicle is its propulsion system, where the electric motor plays a central role in determining overall performance, efficiency, and reliability. Various types of electric motors have been employed in EVs over the years. Initially, DC motors were used due to their simple speed control, but their maintenance requirements and wear issues led to the adoption of induction motors. Squirrel cage induction motors, known for their robustness and low maintenance, became widely used. However, limitations such as low efficiency at partial loads and bulky size restrict their potential in modern compact vehicle designs [3][4].

Brushless DC (BLDC) motors have emerged as a promising alternative, offering several key advantages including high efficiency, compact structure, low maintenance, high power density, and excellent torque-speed characteristics. These motors are electronically commutated, eliminating the need for brushes and mechanical commutators, which enhances reliability and lifespan [5]. Moreover, the advancements in power electronics and sensor technologies have enabled precise control of BLDC motors, making them highly suitable for automotive applications.

The working principle of BLDC motors, commutation methods using Hall sensors or back-EMF sensing, and the control strategies such as DC input voltage variation and PWM control have been widely studied. However, challenges such as torque ripple and poor performance at low speeds, especially in sensorless configurations, remain areas of active research. Minimizing these effects is crucial to achieving smooth

torque delivery, reducing energy losses, and enhancing vehicle performance.

This paper presents a comprehensive review of the evolution of motor technologies in electric vehicles, with a special focus on BLDC motors. It explores their operating principles, control strategies, sensor-based and sensorless techniques, and current challenges. The paper also highlights recent advancements aimed at optimizing motor performance, making BLDC motors a preferred choice for future electric mobility solutions.

I. MODELING OF BLDC MOTOR DRIVE

The Brushless DC (BLDC) motor is an electronically commutated machine characterized by trapezoidal back electromotive force (EMF). In operation, two stator windings are energized during each commutation interval based on rotor position feedback, which is detected using Hall Effect sensors embedded within the stator. These sensors detect the proximity of the rotor's magnetic poles and produce a sequence of high or low logic signals accordingly.

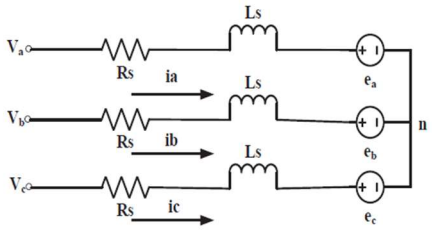

Fig. 1 Equivalent circuit diagram of BLDC Motor

The equivalent circuit model of the BLDC motor is illustrated in Fig. 1. Using this model, the motor's voltage equations in the time domain are expressed as follows:

$$\begin{bmatrix} v_a \\ v_b \\ v_c \end{bmatrix} = \begin{pmatrix} R_s & 0 & 0 \\ 0 & R_s & 0 \\ 0 & 0 & R_s \end{pmatrix} \begin{bmatrix} i_a \\ i_b \\ i_c \end{bmatrix} + \begin{pmatrix} L_s & 0 & 0 \\ 0 & L_s & 0 \\ 0 & 0 & L_s \end{pmatrix} \frac{d}{dt} \begin{bmatrix} i_a \\ i_b \\ i_c \end{bmatrix} + \begin{bmatrix} e_a \\ e_b \\ e_c \end{bmatrix} \quad (1)$$

$$L_s = L_{ss} + L_m \quad (2)$$

In (1) - (7), V & I are the phase voltage and current of the stator and e states the back emf and all are corresponding to 3 phases. L_s is the stator inductance, L_{ss} is the stator leakage inductance, Lm is the mutual inductance per phase. The electromagnetic torque is described as;

$$T_{em}(t) = J\frac{d\omega}{dt} + B\,\omega(t) + T_L(t) \quad (3)$$

Where, T_e is electromagnetic torque, ω is rotor angular velocity, B is viscous friction constant, J is rotor moment of inertia and T_L is load torque. The back emf (a phase) can be described as;

$$e_a = K_e\omega(t) \quad (4)$$

Where, K_e is back emf constant. Laplace domain representation of equations as achieved from (1) and (4) for phase A and can be specified as;

$$V_a(s) = RI_a(s) + sL_aI_a(s) + K_e\Omega(s) \quad (5)$$

$$I_a(s) = \frac{V_a(s) - K_e\Omega(s)}{R + sL_a} \quad (6)$$

Torque T_{em}, explained with back EMF and speed of the motor is described as;

$$T_{em} = \frac{e_ai_a + e_bi_b + e_ci_c}{w} \quad (7)$$

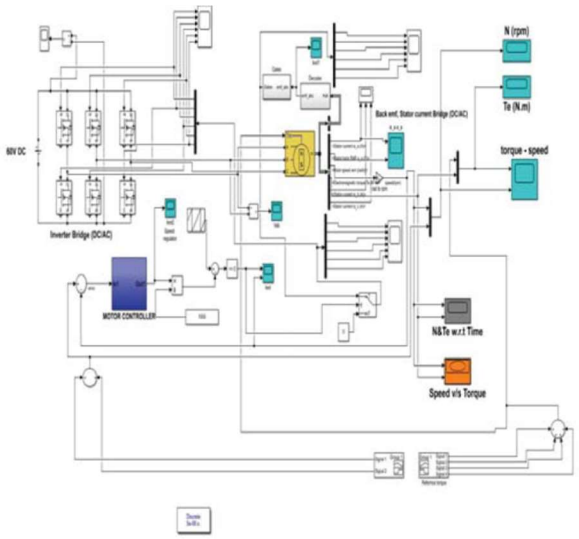

Fig. 2 Simulation diagram of BLDC motor control

A MATLAB/Simulink model of the BLDC motor drive system is developed to simulate closed-loop speed control, as shown in Fig. 2**.** The model incorporates a speed controller, inverter, motor, and Hall sensor-based commutation logic. A range of reference speeds are fed into the controller to analyze dynamic and steady-state motor response.

Hall Sensor Output	Switching Sequences						
	S1	S2	S3	S4	S5	S6	
100	1	0	0	0	0	1	V_{AC}
110	0	0	1	0	0	1	V_{BC}
010	0	1	1	0	0	0	V_{BA}

011	0	1	0	0	1	0	V_{CA}
001	0	0	0	1	1	0	V_{CB}
101	1	0	0	1	0	0	V_{AB}

Table 1 Commutation Sequence of Hall Sensors

The commutation sequence used in the simulation is based on the Hall sensor outputs, which determine the proper pair of phases to energize. Table 1 summarizes the switching sequence corresponding to each Hall sensor combination.

The Brushless DC (BLDC) motor used in this study is rated for a voltage of 60V and a power output of 1000W. It operates at a rated speed of 940 revolutions per minute (rpm) and draws a rated current of 16A. The motor produces a rated torque of 6 Newton-meters (Nm), which is sufficient for driving small electric vehicles such as scooters. The stator phase resistance of the motor is 0.5 Ohm, while the stator phase inductance is measured at 0.2 mH. The voltage or back electromotive force (EMF) constant of the motor is 43.9 V_{peak}/K rpm, and the torque constant is 0.42 Nm/A. These parameters indicate that the motor is well-suited for automotive applications requiring efficient and compact motor performance with reliable torque and speed control.

III. PROPOSED ELECTRIC DRIVE SYSTEM

The Brushless DC (BLDC) motor, a type of permanent magnet synchronous motor, is characterized by its trapezoidal back electromotive force (EMF), resulting from the non-sinusoidal nature of its stator currents. This is primarily due to the use of concentrated windings, which are common in BLDC motor construction. In this work, the motor is used to drive an electric scooter, with the motor integrated directly into the rear wheel hub, eliminating the need for mechanical transmission components. As a result, precise and efficient motor control is essential to achieve optimal vehicle performance.

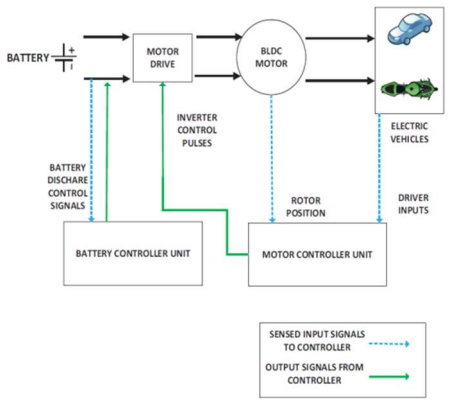

Fig. 3 Block diagram of BLDC motor driving system

The proposed control system is illustrated in Fig. 3, which shows the functional block diagram of the entire drive system. The system consists of two primary control units:

Battery Control Unit (BCU): The BCU is responsible for managing the battery's operation, ensuring safe charging and discharging. It prevents over-discharge of the battery by monitoring the Depth of Discharge (DOD), which is typically limited to 75%. When the battery approaches this threshold, the BCU intervenes to cut off power delivery, thus protecting the battery from damage and extending its lifespan.

Motor Control Unit (MCU): The MCU governs the operation of the BLDC motor, ensuring correct sequencing and speed control. At each commutation step, two of the three motor phases are energized. The rotor position is sensed using Hall Effect sensors placed 120 degrees apart, and based on the feedback, the MCU generates the corresponding PWM pulses. The correct switching sequence, as outlined from data, is critical; any mismatch can lead to erratic motor operation, which is unacceptable in vehicle applications.

The inverter generates a trapezoidal AC output voltage by turning on two switches during each commutation interval. These voltages are applied to the stator windings in synchronization with the rotor position, which creates a rotating magnetic field. The rotor, having permanent magnets, aligns with this field, resulting in torque production and rotation.

Two major speed control techniques are commonly used for BLDC motors:

- **DC Link Voltage Control:** Implemented using a DC-DC converter.
- **PWM Duty Cycle Control:** Where the average voltage applied to the motor is varied by changing the duty cycle of the PWM signals.

In this project, PWM-based speed control is adopted and executed through the MCU. The PWM duty cycle is dynamically adjusted based on the driver input, which is captured through a potentiometer-based throttle (accelerator). As the driver increases throttle, the potentiometer output voltage increases, leading to a corresponding increase in the PWM duty cycle. This results in higher stator currents and, consequently, greater motor speed.

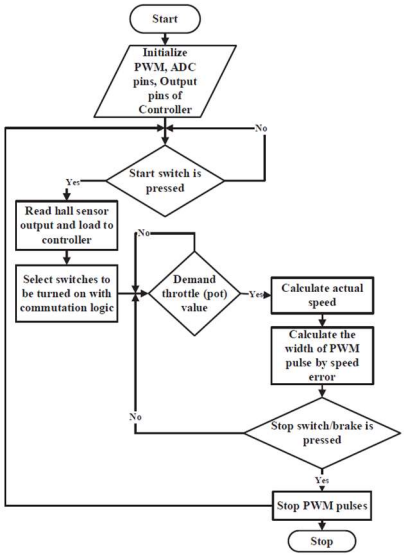

Fig. 4 Flow chart of Motor controller unit (MCU)

Additionally, the MCU responds to stop/run commands from the driver, enabling or disabling motor operation accordingly. The complete control logic is implemented as detailed in the flowchart shown in Fig. 4**.**

This implementation provides a robust and responsive control system suitable for electric scooter applications. Future enhancements may focus on improving torque ripple mitigation, regenerative braking integration, and advanced sensorless control techniques for improved system efficiency and performance.

IV. EFFICIENT CONTROL STRATEGY FOR BLDC MOTOR

The BLDC hub motor selected for this work has a rating of 60V and 1000W, and is employed as the main drive unit for an electric scooter. Since the focus of this study is solely on motor drive control, a constant DC supply of 60V and 4A is provided through a battery charger. The complete hardware setup, including the BLDC hub motor and motor control unit (MCU), is shown in Fig. 5. A three-phase inverter is built using IRFP460 MOSFETs rated at 500V and 20A, selected to match the power requirements of the motor. Gate pulses generated by the MCU are passed through a gate driver circuit, which includes opto-isolator IC 6N137. This circuit isolates the microcontroller from the high-power switching circuit and amplifies the pulse amplitude to effectively drive the MOSFETs.

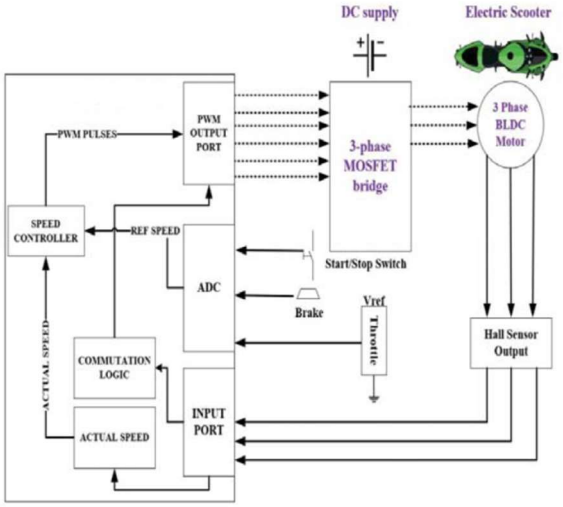

Fig. 5 Functional block diagram of the EV system with MCU

An Arduino Uno board, incorporating the Atmega 328 microcontroller, is used for control implementation. It features 14 digital I/O pins, including six PWM outputs, which are used for motor commutation. The microcontroller receives driver inputs such as throttle (a potentiometer acting as the accelerator), brake, and start/stop signals. Upon receiving the start signal and position feedback from the motor's three embedded Hall sensors, the controller produces appropriate PWM signals according to the commutation logic to initiate motor rotation. The throttle input is continuously read by the controller and used to adjust motor speed accordingly. The brake signal, when activated, instantly halts motor operation by turning off the inverter switches, effectively cutting off voltage supply to the stator windings.

Motor commutation is achieved by driving two of the six inverter switches at any given time, as per the six-step commutation table derived from the Hall sensor outputs. Closed-loop speed control is implemented using a proportional-integral (PI) controller, where the throttle sets the reference speed and the actual motor speed is compared to determine the error. The PI controller, with a proportional gain of 0.008 and an integral gain of 11.5 (tuned using PI tuning methods), adjusts the PWM duty cycle to control the motor's speed accurately.

The key hardware components used in this implementation include the 60V, 1000W BLDC hub motor; a 60V, 4A DC supply; IRFP460 MOSFETs; the 6N137 opto-coupler driver IC; and the Atmega 328 microcontroller. Overall, the motor speed is effectively varied based on the throttle input, while the start/stop and brake inputs provide precise control over motor operation, making the system responsive and well-suited for electric scooter applications.

V. RESULTS

The hardware and simulation results for the BLDC motor drive system demonstrate effective speed control

based on variations in throttle input, and validate the functionality of the implemented control strategy. Figures 6 to 9 illustrate the PWM pulses for inverter switches (specifically S1 and S6) corresponding to the Hall sensor output state 100, under both half and full throttle conditions. In Fig. 6, under half throttle input, the PWM pulses generated for switches S1 and S6 show a reduced duty cycle, corresponding to half the pulse width. The simulation result validating this condition is shown in Fig. 7, where the behavior of the switching and motor response aligns with the hardware output.

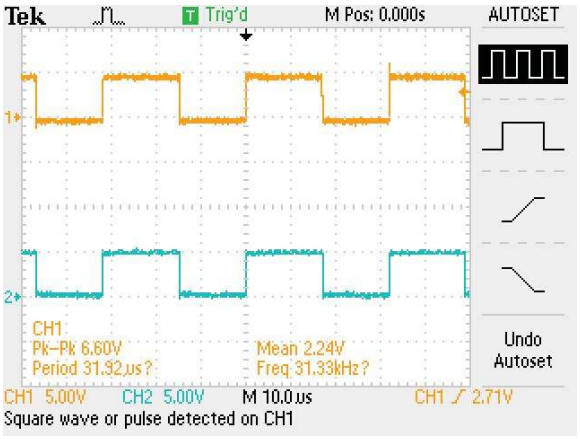

Fig. 6 Experimental results of PWM output pulses of S1 and S6 with half throttle (hall state 100)

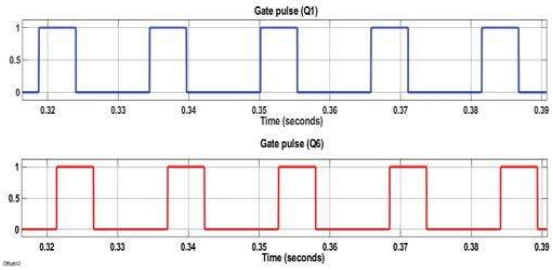

Fig. 7 Results of PWM output pulses of S1 and S6 with half throttle (hall state 100) (Simulation)

With full throttle input, shown in Fig. 8 (hardware) and Fig. 9 (simulation), the pulse width of the PWM signals increases significantly, indicating maximum conduction time for the switches. This results in greater current delivery to the stator windings and hence higher motor speed. The switching pattern remains consistent with the commutation sequence defined for state 100 (switches S1 and S6 ON), ensuring unidirectional rotation. Additionally, reverse operation of the motor was successfully demonstrated by reversing the switching sequence, thereby enabling the potential implementation of a reverse gear at controlled, low speeds a useful feature for electric vehicle applications.

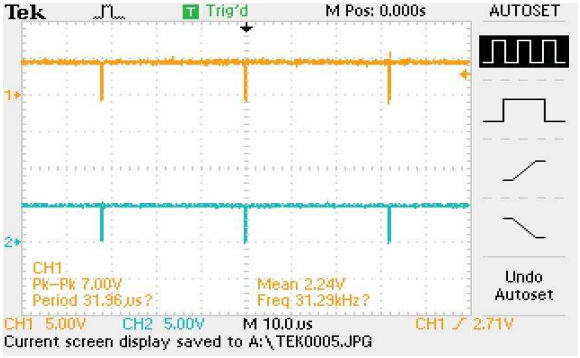

Fig. 8 Experimental results of PWM output pulses of S1 and S6 with full throttle (hall state 100)

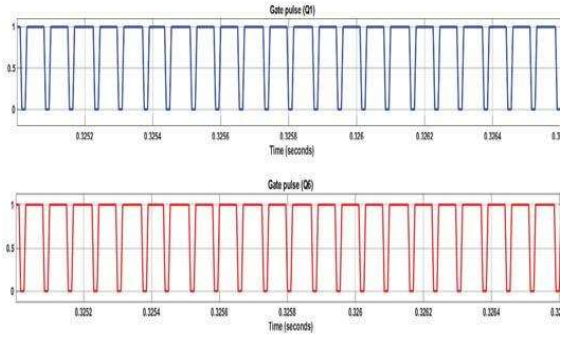

Fig. 9 Results PWM output pulses of S1 and S6 with full throttle (hall state 100) (Simulation)

The experimental back EMF waveform, shown in Fig. 10, and its simulated counterpart in Fig. 11, exhibit a distinct trapezoidal shape with a peak voltage of around 30V, which is characteristic of a BLDC motor with trapezoidal commutation. This confirms the proper functioning of the motor and the accuracy of the commutation logic used in both simulation and hardware.

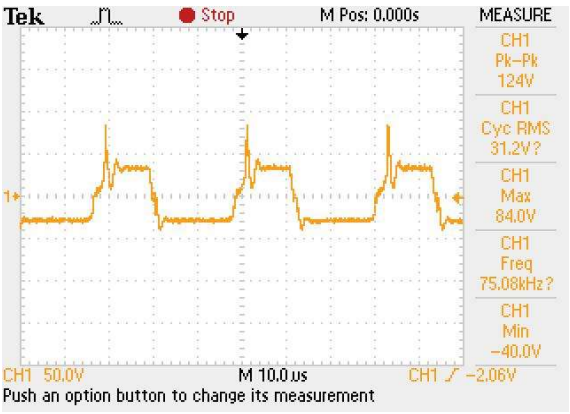

Fig. 10 Experimental results of trapezoidal back EMF voltage

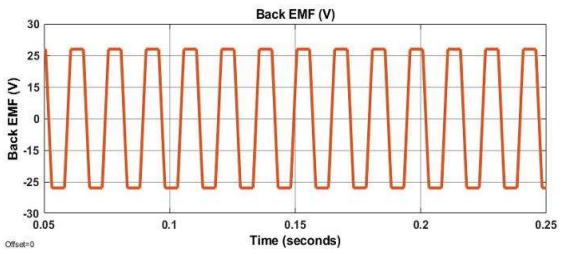

Fig. 11 Result of trapezoidal back EMF voltage (Simulation)

Fig. 12 presents the speed response of the motor under dynamic load conditions. A load torque of 6 Nm (equal to the motor's rated torque) is applied between 0.25 and 0.4 seconds. During this interval, the motor operates at the rated speed of 940 rpm, but noticeable ripples are observed in the speed response due to torque ripple generated by non-ideal commutation. When the load torque is removed, the motor speed returns to the reference value set by the throttle input. These torque ripples, visible in both the speed response and back EMF voltage (as spikes in Fig. 10), can impact motor efficiency and smoothness of operation.

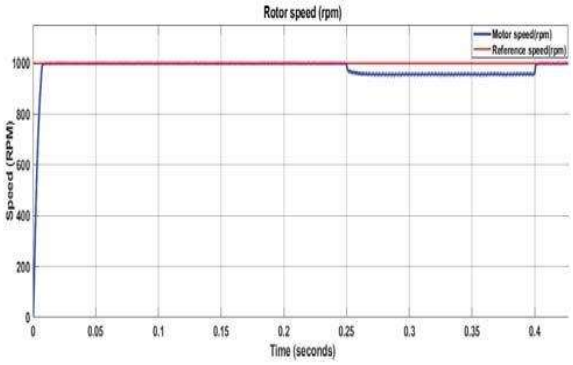

Fig. 12 Results of speed of BLDC motor (rated load torque of 6 Nm at 0.25 to 0.4 sec (940 rpm) (Simulation)

To mitigate these effects and enhance performance, advanced torque ripple reduction techniques can be incorporated in future designs. Such improvements would lead to more stable motor operation, higher efficiency, and better overall performance in electric vehicle applications.

VI. CONCLUSION

In this work, a Brushless DC (BLDC) hub motor control system has been successfully modeled, simulated, and implemented for electric vehicle propulsion. The motor's behavior was first analyzed using mathematical modeling and simulated in MATLAB with a closed-loop speed control mechanism, enabling precise tracking of vehicle speed based on driver inputs. The system was further validated through hardware implementation using a microcontroller, which generated appropriate PWM signals for motor commutation and controlled the motor operation effectively in real-time.

The results from both simulation and hardware experimentation confirm that the proposed drive system offers reliable and efficient performance for electric vehicle applications. The motor demonstrated stable operation under varying speed conditions and responded well to control commands, proving the viability of the system for real-world use. The capability for reverse direction operation was also discussed, showing the system's flexibility through commutation sequence reversal.

Additionally, the foundation has been laid for future improvements such as advanced control techniques to reduce torque ripple and enhance dynamic performance. The proposed BLDC motor control system is compact, cost-effective, and scalable, making it a promising solution for the evolving needs of the electric transportation sector.

References

[1] Electric Vehicle Technology Explained, James Larminie Oxford Brookes University, Oxford, UK John Lowry Acenti Designs Ltd., UK

[2] A. Emadi, Y. L. Lee, and R. Rajashekara, *"Power electronics and motor drives in electric, hybrid electric, and plug-in hybrid electric vehicles"*, IEEE Trans. Ind. Electron., vol. 55, no. 6, pp. 2237–2245,Jun. 2008.

[3] C. Chakraborty and Y. Hori, *"Fast Efficiency Optimization Techniques for the Indirect Vector-Controlled Induction Motor Drives"*, IEEE Trans. Ind. Applicat, vol. 39, no. 4, pp1070-1076, July/August 2003.

[4] R.Yanamshetti, S.S.Bharatkar, D.Chatterjee and A.K.Ganguli, *"A Dynamic Search Technique For Efficiency Optimization For Variable Speed Induction Machine"* in Proc. IEEE ICIEA'09, Xian, China, 2009, pp 1038-1042.

[5] C. L. Xia, Permanent Magnet Brushless DC Motor Drives and Controls. Beijing, China: Wiley, 2012.

[6] Y. Chen, C. Chiu, Y. Jhang, Z. Tang, and R. Liang, *"A driver for the singlephase brushless DC fan motor with hybrid winding structure"*, IEEE Trans. Ind. Electron., vol. 60, no. 10, pp. 4369–4375, Oct. 2013.

[7] X. Huang, A. Goodman, C. Gerada, Y. Fang, and Q. Lu, *"A single sided matrix converter drive for a brushless dc motor in aerospace applications"*, IEEE Trans. Ind. Electron., vol. 59, no. 9, pp. 3542–3552, Sep. 2012.

[8] W. Cui, Y. Gong, and M. H. Xu, *"A permanent magnet brushless DC motor with bifilar winding for automotive engine cooling application"*, IEEE Trans. Magn., vol. 48, no. 11, pp. 3348–3351, Nov. 2012.

[9] C. C. Hwang, P. L. Li, C. T. Liu, and C. Chen, *"Design and analysis of a brushless DC motor for applications in robotics"*, IET Elect. Power Appl., vol. 6, no. 7, pp. 385–389, Aug. 2012.

[10] G. Liu, C. Cui, K. Wang, B. Han and S. Zheng, *"Sensorless Control for High-Speed Brushless DC Motor Based on the Line-to-Line Back EMF"*, in IEEE Transactions on Power Electronics, vol. 31, no. 7, pp.4669-4683, July2016.

[11] S. Manglik, S. Sundeep and B. Singh, *"Brushless DC motor based ceiling fan using buck-boost converter"*, 2016 IEEE 7th Power India International Conference (PIICON), Bikaner, 2016, pp. 1-6.

[12] R. Bhosale, W. Warshe, M. P. Shreelakshmi, P. Arlikar, A. K. Prakash and V. Agarwal, *"Performance comparison of Two PWM techniques applied to BLDC motor control"*, 2018 International Conference on Power, Instrumentation, Control and Computing (PICC), Thrissur, 2018, pp. 1-6.

[13] Y. Liu, Z. Q. Zhu, and D. Howe, *"Direct Torque Control of Brushless DC Drives with Reduced Torque Ripple"*, IEEE Trans. Ind. Appl., vol.41, no. 2, pp. 599–608, Mar. /Apr. 2005.

[14] D. K. Kim, K. W. Lee, and B.-I. Kwon, *"Commutation torque ripple reduction in a position sensorless brushless DC motor drive"*, IEEE Trans.Power Electron., vol. 21, no. 6, pp. 1762–1768, Nov. 2006.

[15] A. G. de Castro, W. C. A. Pereira, T. E. P. de Almeida, C. M. R. de Oliveira, J. Roberto Boffino de Almeida Monteiro and A. A. de Oliveira, *"Improved Finite Control-Set Model-Based Direct Power Control of BLDC Motor With Reduced Torque Ripple"*, in IEEE Transactions on Industry Applications, vol. 54, no. 5, pp. 4476-4484, Sept.- Oct.2018.